Multicenter Matrix-Assisted Laser Desorption/Ionization Mass Spectrometry Imaging (MALDI MSI) Identifies Proteomic Differences in Breast-Cancer-Associated Stroma

Dekker, T.J.A.; Balluff, B.D.; Jones, E.A.; Schone, C.D.; Schmitt, M.; Aubele, M.; ... ; McDonnell, L.A.

Journal of proteome research

Article

pubs.acs.org/jpr

Multicenter Matrix-Assisted Laser Desorption/Ionization Mass Spectrometry Imaging (MALDI MSI) Identifies Proteomic Differences in Breast-Cancer-Associated Stroma

Tim J. A. Dekker,[†,‡] Benjamin D. Balluff,[§] Emrys A. Jones,[§] Cédrik D. Schöne,[∥] Manfred Schmitt,[⊥] Michaela Aubele,[#] Judith R. Kroep,[‡] Vincent T. H. B. M. Smit,[▽] Rob A. E. M. Tollenaar,[‡] Wilma E. Mesker,[‡] Axel Walch,[∥] and Liam A. McDonnell*[,§]

[†]Department of Clinical Oncology, Leiden University Medical Center, Leiden, The Netherlands

[‡]Department of Surgery, Leiden University Medical Center, Leiden, The Netherlands

[§]Center for Proteomics and Metabolomics, Leiden University Medical Center, Einthovenweg 20, 2333 ZC Leiden, The Netherlands

[∥]Research Unit Analytical Pathology, Helmholtz Zentrum München - German Research Center for Environmental Health, Neuherberg, Germany

[⊥]Department of Obstetrics and Gynecology, Klinikum rechts der Isar, Technische Universität München, Munich, Germany

[#]Institute of Pathology, Helmholtz Zentrum München - German Research Center for Environmental Health, Neuherberg, Germany

[▽]Department of Pathology, Leiden University Medical Center, Leiden, The Netherlands

ABSTRACT: MALDI mass spectrometry imaging (MSI) has rapidly established itself as a powerful biomarker discovery tool. To date, no formal investigation has assessed the center-to-center comparability of MALDI MSI experiments, an essential step for it to develop into a new diagnostic method. To test such capabilities, we have performed a multicenter study focused on biomarkers of stromal activation in breast cancer. MALDI MSI experiments were performed in two centers using independent tissue banks, infrastructure, methods, and practitioners. One of the data sets was used for discovery and the other for validation. Areas of intra- and extratumoral stroma were selected, and their protein signals were compared. Four protein signals were found to be significantly associated with tumor-associated stroma in the discovery data set measured in Munich. Three of these peaks were also detected in the independent validation data set measured in Leiden, all of which were also significantly associated with intratumoral stroma. Hierarchical clustering displayed 100% accuracy in the Munich MSI data set and 80.9% accuracy in the Leiden MSI data set. The association of one of the identified mass signals (PA28) with stromal activation was confirmed with immunohistochemistry performed on 20 breast tumors. Independent and international MALDI MSI investigations could identify validated biomarkers of stromal activation.

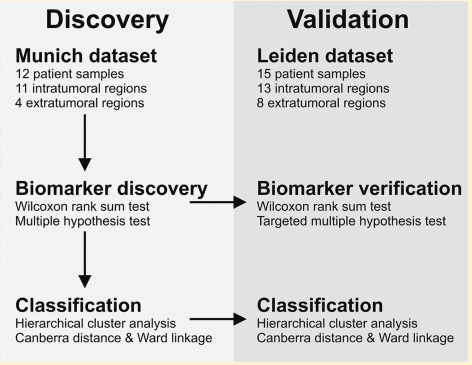

KEYWORDS: *tumor-associated stroma, breast cancer, MALDI imaging mass spectrometry, MSI, multicenter study, proteomics*

1. INTRODUCTION

1.1. Tumor-Associated Stroma

Tumor-associated stroma has recently received increased attention due to the effect of stroma on tumor growth, patient prognosis, and occurrence of metastases.[1] Arguably the most frequently reported marker associated with cancer associated fibroblasts (CAFs) and stromal activation is α-smooth muscle actin (α-SMA). α-SMA is also associated with myofibroblasts involved in wound healing, myoepithelial cells, and various other cell types, which hinders the use of this protein as a specific marker for activated fibroblasts. Sugimoto et al. showed that the tumor-associated stroma is very heterogeneous and that α-SMA lacks sufficient sensitivity to identify all CAFs.[2] Novel markers for tumor-associated stromal activation are needed to identify novel mechanisms of stromal activation and proper definition of CAFs.

1.2. Matrix-Assisted Laser Desorption/Ionization Mass Spectrometry Imaging

Matrix-assisted laser desorption/ionization mass spectrometry (MALDI MS) constitutes a powerful biomarker discovery tool because it can generate biomolecular profiles containing hundreds of biomolecular ions directly from tissues.[3] Spatially

Special Issue: Proteomics of Human Diseases: Pathogenesis, Diagnosis, Prognosis, and Treatment

Received: March 12, 2014
Published: April 24, 2014

   dx.doi.org/10.1021/pr500253j | J. Proteome Res. 2014, 13, 4730−4738

correlated analysis by mass spectrometry imaging (MSI), can simultaneously record the distribution of each of these ions.[4,5] Following a MALDI MSI experiment, the tissue can be stained with hematoxylin and eosin (H&E) and a high-resolution digital image of the stained tissue aligned with the MALDI MSI data set. Following histopathological analysis, MALDI MS biomolecular profiles of specific histological entities can be extracted[6] and then used to identify biomarkers or biomarker profiles. Statistical analysis of the data is performed to identify candidate biomarkers, which are then validated against an independent patient cohort and if possible by using an orthogonal molecular test (e.g., immunohistochemistry (IHC) for protein biomarkers).[7]

Published results indicate that MALDI MSI has great potential to develop into a valuable diagnostic technique that can complement established histological and histochemical methods, provided the biomarkers or classifiers can be robustly reproduced in different biomedical centers. While very recent investigations have included patient tissues from additional institutions to demonstrate the broader applicability of the classifier,[8,9] these have not addressed the crucial role of user variability. User variability in MSI has not been quantified, but a cursory comparison of the methods undertaken as part of a wide European MSI network has indicated substantial differences between different practitioners and laboratories. Differences in tissue sampling and MALDI MSI tissue preparation are known to affect MALDI MSI performance;[10] the choice of matrix, solvent, addition of cofactors, and matrix crystallization rate affect the mass spectral signatures detected in MALDI[11] and MALDI MSI.[12] Deininger et al. have demonstrated that total-ion-count normalization can compensate for small differences that may arise from minor fluctuations in matrix coating or laser intensity.[13] Here we demonstrate that provided they are detected in both centers the biomarkers reported by MALDI MSI can be resilient to differences in tissue preparation protocols.

1.3. Study Objectives

To identify novel markers for stromal activation in breast cancer and address user variability when using MSI, we used this method independently in two centers to measure and compare proteomic signals from activated, intratumoral stroma with quiescent, extratumoral stroma derived from tumors analyzed in both Munich (N = 12) and Leiden (N = 18). After this initial experiment, results were validated using IHC (N = 20).

2. MATERIAL AND METHODS

2.1. Samples

Frozen breast cancer tissues of the ductal subtype from two institutes, namely, the Klinikum rechts der Isar, Technische Universität München, Germany, and Leiden University Medical Center, The Netherlands, were used in this study. All tissues were snap-frozen after surgical removal and stored in liquid nitrogen freezers until use. The tumor tissues from the archives in Munich were analyzed after written patient consent was obtained. The use of the material was approved by the ethics committee of the Faculty of Medicine of the Technische Universität München. All tumors analyzed in Leiden were acquired during routine patient care. According to Dutch law, these can be freely used after anonymizing the tissues, provided these are handled according to national ethical guidelines ("Code for Proper Secondary Use of Human Tissue", Dutch Federation of Medical Scientific Societies). A third set of breast cancer patient samples for immunohistochemical validation was available, all of which were excised in Leiden and subsequently stored as formalin-fixed paraffin-embedded tissue blocks. Table 1 details the clinical characteristics of all sample collections.

Table 1. Clinical Characteristics of Analyzed Patient Tissue Collections

	Munich set MALD MSI (N = 12)	Leiden set MALD MSI (N = 18)	IHC validation set (N = 20)
pT1	8	3	4
pT2	0	9	11
pT3+pT4	3	6	5
Unknown	1	0	0
pN0	5	9	6
pN+	5	9	14
Unknown	2	0	0
Grade			
I,II	11	4	14
III	1	14	6
Estrogen receptor status			
Positive	12	0	12
Negative	0	18	7
Unknown	0	0	1
Human epidermal growth factor receptor 2 status			
Positive	1	0	3
Negative	11	18	6
Unknown	0	0	11

2.2. MALDI MSI

Both fresh-frozen ductal-type breast cancer tissue cohorts were measured completely independently. Tissues from the Klinikum rechts der Isar were measured by Cedrik Schöne at the Institute for Pathology, Helmholtz Zentrum München. Tissues from Leiden University Medical Center were measured by Tim Dekker at the Center for Proteomics and Metabolomics, Leiden University Medical Center. Both sets of experiments were performed using local MALDI MSI protocols.

Tissue sections were sectioned at 12 μm with a cryomicrotome (Leica, Germany) and transferred to precooled conductive indium−tin-oxide coated glass slides (Bruker Daltonik, Bremen, Germany). After sectioning, the tissues in Munich were washed with 70 and 100% ethanol solutions. In Leiden, washing was performed via serial washing steps in 60 and 100% methanol. Both centers used sinapinic acid as MALDI matrix, which was deposited onto the tissues using an automated spraying device (ImagePrep, Bruker Daltonik). In Munich, the matrix solution was 10 mg/mL sinapinic acid in 3:2:0.01 acetonitrile/H_2O/trifluoroacetic acid, whereas in Leiden the matrix solution was 10 mg/mL sinapinic acid in 7:3 methanol/H_2O.

MALDI MSI data acquisition was performed with an Ultraflex III MALDI-ToF/ToF mass spectrometer in Munich and an UltrafleXtreme MALDI-ToF/ToF in Leiden, both of which were supplied by Bruker Daltonik. Spatial resolution was set to 70 μm for the Munich measurements and to 150 μm for the Leiden experiments. Positive ions were detected in the mass range m/z 2520−25 100 with a digitization rate of 0.1 G/s (Munich) and m/z 2000−28000 with a digitization rate of 0.5 G/s (Leiden). All mass spectra were externally calibrated using the protein calibration standard I from Bruker Daltonics, which contains insulin, ubiquitin I, cytochrome c, and myoglobin.

After data acquisition, all slides were washed with 70% ethanol solution and stained via conventional H&E staining protocols. H&E stained slides were then scanned with a Mirax

dx.doi.org/10.1021/pr500253j | J. Proteome Res. 2014, 13, 4730−4738

Table 2. Summary of the Different MALDI MSI Methods

	Munich	Leiden
washing	70% ethanol (1 min), 100% ethanol (1 min)	60% methanol (1 min), 100% methanol (1 min)
matrix (deposition system)	sinapinic acid (image prep device)	sinapinic acid (image prep device)
mass spectrometer (mode)	Ultraflex III (positive linear)	UltrafleXtreme (positive linear)
m/z range	2520−25100	2000−28000
lateral resolution	70 μm	150 μm
digitization rate (G/s)	0.1	0.5
H&E coregistration	same slide	same slide
maximum peak shift (ppm)	1000	1000
% match to calibrant peaks	20	20

DESK digital slide scanner (Munich) or a Leica Ariol digital slide scanner (Leiden), and the optical images were aligned with the MALDI MSI data sets using the data acquisition and data analysis software FlexImaging (v3.0, Bruker Daltonik). Table 2 summarizes the different methodological approaches.

2.3. MALDI MSI Data Processing and Analysis

Using the MALDI MSI software, FlexImaging regions of extratumoral or intratumoral stroma were defined based on the aligned histological images to compare protein signatures of the cancer-associated stroma and normal, quiescent stroma. This is based on the assumption that the stroma that is directly adjacent to the tumor has been activated by tumor epithelial cells (via soluble factors like TGF-β, PDGF, and others) and will result in measurable differences in protein expression. Stromal areas from within the primary tumors were selected as areas of tumor-associated stroma. Because only tumor tissue and no normal breast specimens were available, stroma was characterized as physiological quiescent (extratumoral) if it was found outside the contours of the primary tumor (while still in the same resection specimen) and with a morphological aspect of physiologic stroma. The MALDI MSI data corresponding to the extratumoral and intratumoral stroma regions were then selected and loaded into the ClinProTools software (Bruker Daltonik). Prior to statistical analysis, all mass spectra were smoothed using the Savitsky−Golay algorithm with a width of 2.0 m/z and five cycles, baseline subtracted with the top-hat algorithm (10% width), normalized to each spectrum's total ion count, and aligned to common mass spectral peaks using a maximum tolerance of 1000 ppm and 20% peak-match. All null spectra and those that could not be aligned were excluded from further analysis.

2.4. Statistical Analysis

To identify mass-spectral peaks that were differentially detected in tumor-associated stroma compared with physiological stroma, we evaluated differences in peak intensities using the Wilcoxon rank-sum test. Significant peaks were defined as those with P values <0.05. The Munich data set was treated as the discovery set, and all reported P values include the Benjamini−Hochberg multiple-hypothesis test correction.[14] The Leiden data set was treated as the independent verification set. Accordingly, multiple-hypothesis testing adjustment was performed only on these targeted m/z signals. To assess the capacity for differentiating samples based on a combined proteomic pattern, we used the most discriminating signals to perform a hierarchical clustering analysis. This was carried out with the R software package (R Foundation for Statistical Computing, Vienna, Austria) using the Canberra distance metric and the Ward linkage. Furthermore, the data from both centers were combined by a meta-analysis, assuming random effects between centers ("meta" package in R). The summary statistic was calculated using the standardized mean difference of the ranked MALDI MSI data (to mimic Wilcoxon-rank-sum test).

Statistical analysis of the results from the IHC experiments was done using a paired t test, as both intra- and extratumoral stromal regions could be found within the analyzed samples.

2.5. Immunohistochemistry

IHC was performed on 4 μm thick formalin-fixed paraffin-embedded tissue slides of a cohort of invasive breast cancer tissues. Tissues were sectioned on a microtome and subsequently dried overnight at 37 °C and stored in the refrigerator until IHC procedure. Deparaffinization, rehydration, and antigen retrieval were performed with the PT link machine (according to manufacturer's instructions, DAKO, Denmark) by heating for 10 min at 90 °C in target retrieval solution (low-pH, DAKO, Denmark). Following this procedure, slides were subjected to a 20 min incubation with hydrogen peroxide solution to block endogenous peroxidase activity. Slides were subsequently blocked by incubation with excess volume PBS (phosphate-buffered saline) with 1% albumin solution. Tissue sections were incubated at room temperature in 150 μL of solution of polyclonal rabbit antibodies directed at the c-term region of PA28 (Invitrogen), diluted at a ratio of 1:500 in PBS with 1% albumin. After overnight incubation, peroxidase-labeled polymer conjugated secondary antirabbit antibody (EnVision, DAKO, Denmark) was added and incubated for 30 min at room temperature. DAB (3,3′-diaminobenzidine) solution (DAKO, Denmark) was then added to visualize antigen−antibody complexes via 5 min of incubation. Slides were counterstained with hematoxylin and dehydrated via increasing alcohol solutions and xylene. Images of the IHC-stained sections were captured via light microscopy (Leica DMRB, Leica, Germany). Areas were randomly selected from intratumoral and extratumoral stromal regions. Quantitative evaluation of the PA28-positive signals per pixel was performed using the ImageJ data analysis software (WS Rasband, http://rsb.info.nih.gov/ij/). Using the red−green−blue (RGB) threshold tool DAB-positive particles were counted and analyzed. To determine the total number of stromal cells, we converted the image to 8-bit and used a threshold tool to highlight the total number of cells. The final read out parameter was the ratio of DAB-positive cells to the total number of cells.

3. RESULTS

3.1. MALDI MSI Analysis of Stromal-Tissues

The aim of the study was to identify markers for stromal activation in breast cancer tissues and to assess if the markers

dx.doi.org/10.1021/pr500253j | J. Proteome Res. 2014, 13, 4730−4738

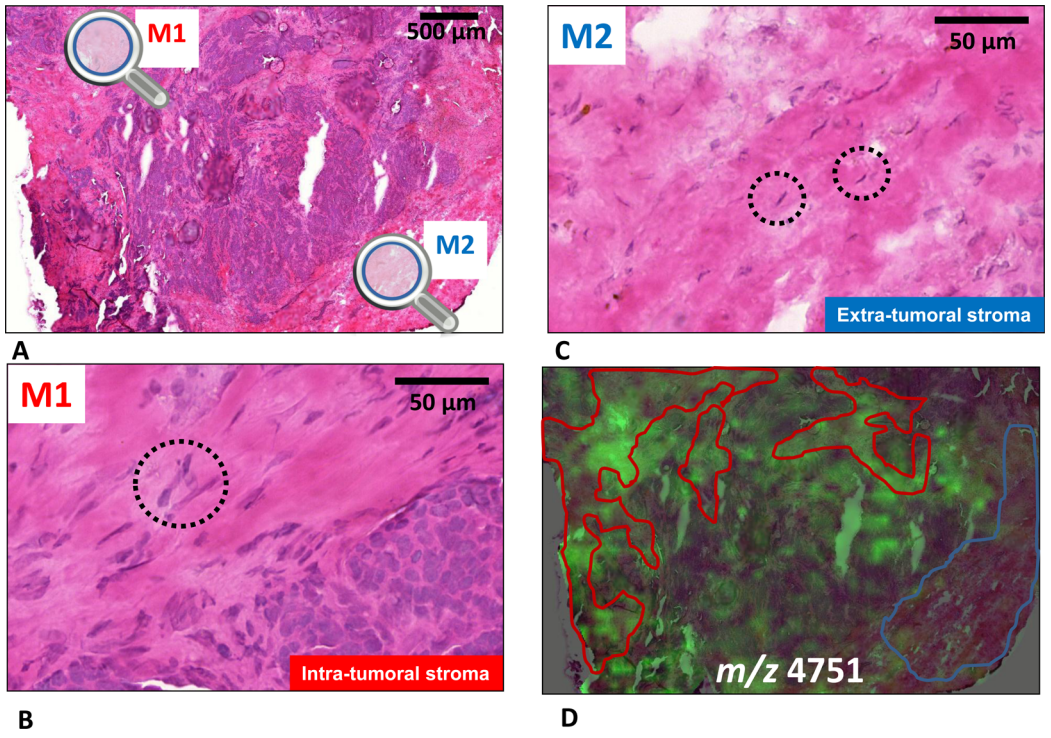

Figure 1. Comparison of the signal intensity of m/z 4751 in a breast tumor. (A) H&E image of a MALDI-MSI-analyzed tumor that contains intratumoral, morphologically activated stromal tissues (panel B, with activated fibroblasts marked with the dotted circle) and extratumoral, morphologically normal stromal tissues (panel C, with normal-appearing fibroblasts marked with the dotted circles). Panel D shows that the signal for m/z peak 4751 is present in the intratumoral stroma (lined in red) but not the physiological stroma (lined in blue).

could be independently validated using independently measured samples (different tissue collection, different instrument, different sample preparation protocol, and different operator). Figure 1A shows an H&E-stained specimen that contained both intratumoral and extratumoral stroma and was analyzed via MALDI MSI. Areas of stroma from within the borders of the invasive tumor adhered to morphological characteristics commonly seen in tumor-associated stromal tissues (myofibroblast differentiation and proliferation and fibrotic stromal reaction, Figure 1B). The areas that were seen outside of the tumor contour were verified to be morphologically similar to physiologic stroma (Figure 1C). The protein at m/z 4751, previously identified[15] as a shortened form of thymosin β4, can be seen to localize to the intratumoral stroma (Figure 1D), confirming that MALDI MSI can indeed identify protein signals located to this compartment and not the stroma with a morphologically normal aspect outside of the tumor. Figure 2 summarizes the basic study design, in which one data set (tissue samples from Munich, measured in Munich using the local sample preparation protocol) was used as a discovery data set and which was then validated using a completely independent data set (tissue samples from Leiden, measured in Leiden using the local sample preparation protocol).

3.2. Selection of Intra- and Extra-Tumoral Stromal Regions

Stroma regions were selected from 12 different resection specimens of the Munich data set, which resulted in 11 areas of intratumoral stroma and 4 areas of extratumoral stroma. (The morphological appearance of all regions was verified on the aligned histological images.) In the Leiden data set, 8 regions of extratumoral stroma and 13 regions of intratumoral stroma were selected from 18 different resection specimens. The

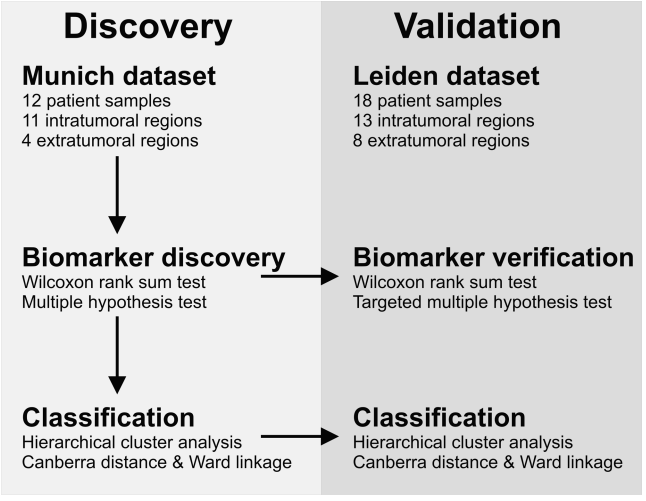

Figure 2. Summary of the study design.

clinico-pathological characteristics for both tissue cohorts are summarized in Table 1.

3.3. Detection of Stroma-Associated Signals in Munich and Leiden Data Sets

Wilcoxon rank-sum tests were performed to identify differences in protein expression between intra- and extratumoral stroma. In the Munich data set, four peaks displayed a significantly higher intensity in intratumoral stroma ($P < 0.05$), namely, m/z 4751, m/z 6279, m/z 9752, and m/z 8619 (all $P = 0.04$). Figure 3A depicts the bar-and-whiskers plots of peak intensities, demonstrating the effective separation of extratumoral and intratumoral stroma. The Leiden data set included three of the four peaks within a 1000 ppm tolerance and which could be

dx.doi.org/10.1021/pr500253j | J. Proteome Res. 2014, 13, 4730−4738

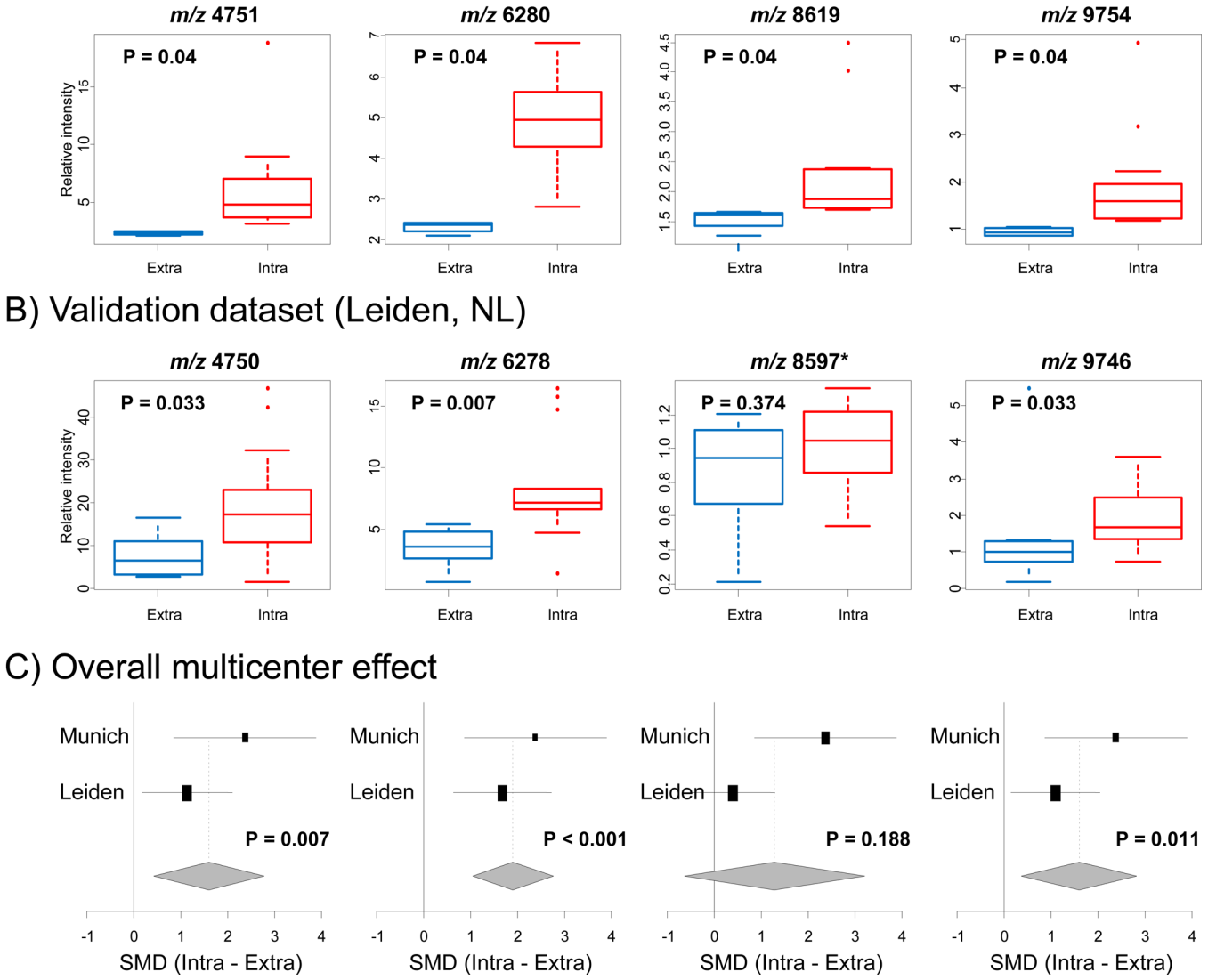

Figure 3. (A) Bar-and-whiskers plots of the four peaks that were associated with the intratumoral stroma in the samples analyzed in Munich. (B) Bar-and-whiskers plots of the same peaks in the Leiden data set. *The peak at 8597 was not detected in this data set. (C) The overall multicenter effect of the four peaks in both data sets.

aligned with the Munich data set by recalibrating the mass spectra. Prior to mass spectral alignment, the m/z_{Munich} 4751 peak was detected at m/z_{Leiden} 4750, the m/z_{Munich} 6279 peak at m/z_{Leiden} 6277, and the m/z_{Munich} 9752 peak at m/z_{Leiden} 9745. The remaining peak, m/z_{Munich} 8619, was not detected in the Leiden cohort in either the extratumoral or intratumoral stroma. The statistically significant association with intratumoral stroma ($P < 0.05$) observed in the Munich data set could be validated for the three peaks detected in the Leiden data set, namely, m/z 4751 ($P = 0.033$), m/z 6279 ($P = 0.007$), and m/z 9752 ($P = 0.033$) (Figure 3B). The forest plot in Figure 3C shows the overall multicenter effect for those four peaks, as determined by meta-analysis, which summarizes their general validity.

3.4. Cluster Analysis of Munich and Leiden Data Sets

The combined pattern of these peaks was then subjected to hierarchical clustering to assess their combined ability to discriminate intratumoral from extratumoral stroma. Hierarchical clustering orders the data according to the similarity between each (stroma) sample's expression profile (rows) and between each protein (columns). This was first performed on the Munich data set using the four statistically significant biomarker peaks (m/z 4751, m/z 6279, m/z 9752, m/z 8619) (Figure 4A). The dendrogram to the left of the heatmap shows that the extra tumoral stoma profiles were distinctly and consistently different than all intratumoral stromal profiles and so clustered separately with a 100% classification accuracy. The same clustering was then also performed on the Leiden data set using the three independently validated peaks (m/z 4751, m/z 6279, and m/z 9752), which resulted in a classification accuracy of 80.9% (Figure 4B). For identifying intratumoral stromal regions, this classifier had a sensitivity of 69%, a specificity of 100%, and a positive predictive value of 100%.

3.5. Provisional Protein Identity Assessment

Two out of the three mass spectral peaks that were independently validated in this study have been previously

dx.doi.org/10.1021/pr500253j | J. Proteome Res. 2014, 13, 4730−4738

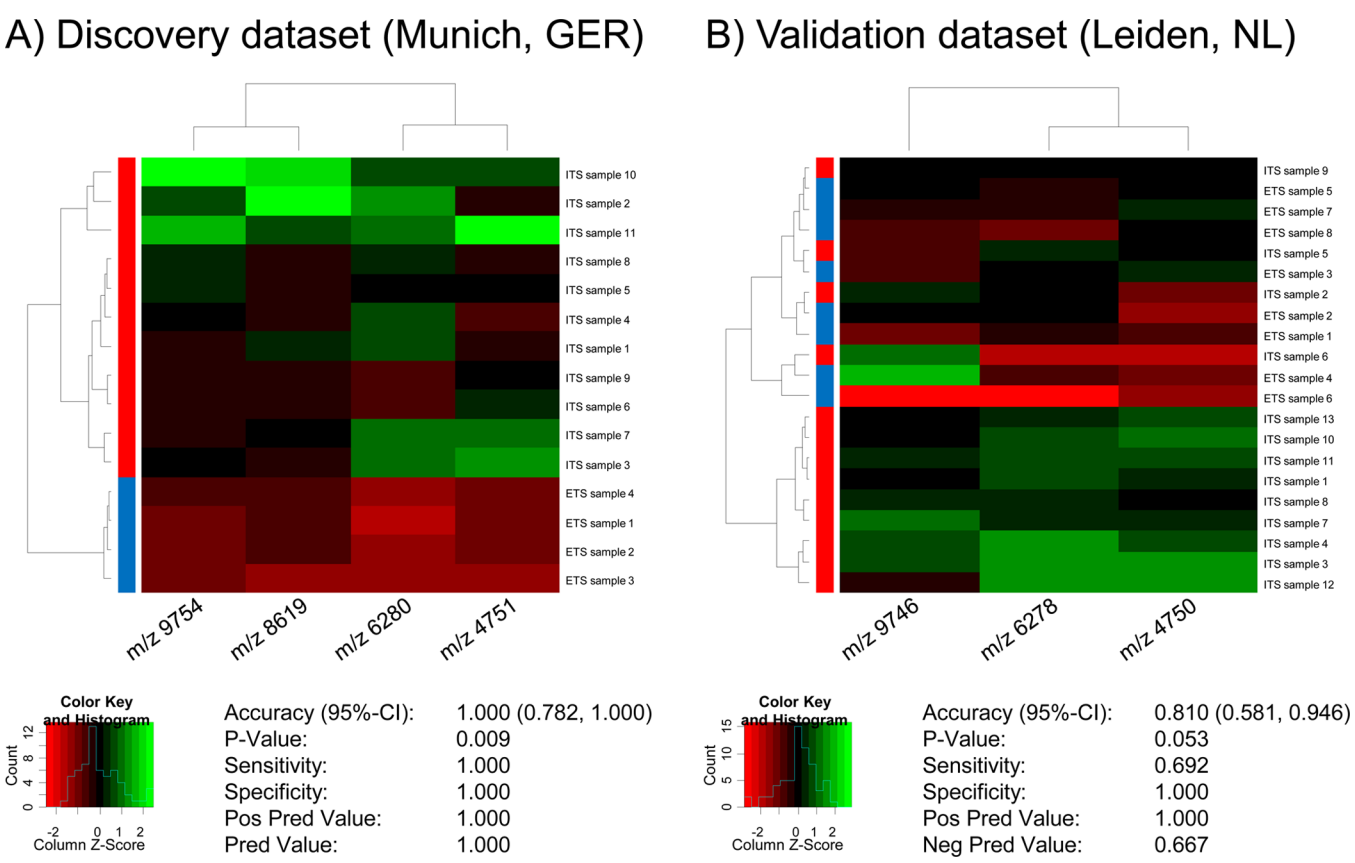

Figure 4. (A) Hierarchical clustering of the samples in the Munich data set, achieving a 100% correct classification of all stromal samples. ITS, intratumoral stroma; ETS, extratumoral stroma. (B) Hierarchical clustering of the samples in the Leiden data set, achieving a 80.9% correct classification of all stromal samples (ITS, intratumoral stroma; ETS, extratumoral stroma).

detected in other MALDI MSI studies and hence are also listed in the MALDI MSiMass list identification database.[16] The peak detected at m/z_{Leiden} 4570 (m/z_{Munich} 4751) was previously detected by Hardesty et al. in a study investigating prognostic biomarkers for metastatic melanoma, which identified this peak as a cleaved form of thymosin β4.[15] The peak identified in our study at m/z_{Leiden} 9745 (m/z_{Munich} 9752) has been previously shown to be the c-terminal fragment of PA28, an 11S proteasome activator complex and to correspond to tumor stage in ovarian cancer.[17]

3.6. Immunohistochemistry Validation

To validate PA28 as a marker for stromal activation, a series of invasive breast cancers (Table 1) were stained with PA28 antibodies to compare the expression of this marker in the extracellular and the intracellular stroma via digital image analysis. The number of cells with PA28 expression was determined and divided by the total number of pixels. These values were subsequently compared via a paired t test. An increased expression of PA28 in intratumoral stroma (Figure 5D) compared with extracellular stroma (Figure 5E) was found (difference of the means = 63.25 per pixel ($\times 10^6$), 95% CI: 30.77−95.73, P = 0.001), which confirms the observations in the MALDI MSI experiments (Figure 5A−C). Because some PA28 staining was also observed in extratumoral stromal cells, the increased PA28 signals inside the tumor-associated stroma might be explained not by upregulation of this marker but simply by the increased number of stromal cells because this is one of the characteristics of stromal activation. To investigate this further, we determined the relative proportion of PA28 positive cells among the total number of stromal cells in the extratumoral and intratumoral tissues. The relative number of PA28 stromal cells was elevated in the intratumoral stroma (51.2% in the intratumoral stromal cells compared with 31.7% in the extratumoral stromal cells, 95% CI: 8.1−30.9, P = 0.003, Figure 5F). These data suggest that stromal activation is not only accompanied by an increased number of PA28 positive cells but also with an increased proportion of PA28 cells and that increased expression of this marker in fact indicates activated stromal cells. Because PA28 previously has mostly been described as a protein involved in immune response, we investigated whether PA28 expression was increased in both the tumor-associated inflammatory cells and tumor-associated fibroblasts. ImageJ was used to determine the shape of the PA28-positive cells in the intracellular and extracellular stromal regions in the five tumors that had the highest expression of PA28. Particles with an aspect ratio of more than 2.5 were determined to be fibroblasts. In all five tumors, an increased proportion of fibroblasts was observed in the intratumoral stroma (average difference between intratumoral and extratumoral stroma was 30.2% of stromal cells (range 13.0−68.0%), indicating that increased expression of PA28 is one of the characteristics of stromal activation).

4. DISCUSSION

Using MALDI MSI, we have identified protein signals characteristic for tumor-associated stroma. Previous studies assessing transcriptional activity in microarrays have shown differences in tumor-associated stroma. For instance, Navab et

dx.doi.org/10.1021/pr500253j | J. Proteome Res. 2014, 13, 4730−4738

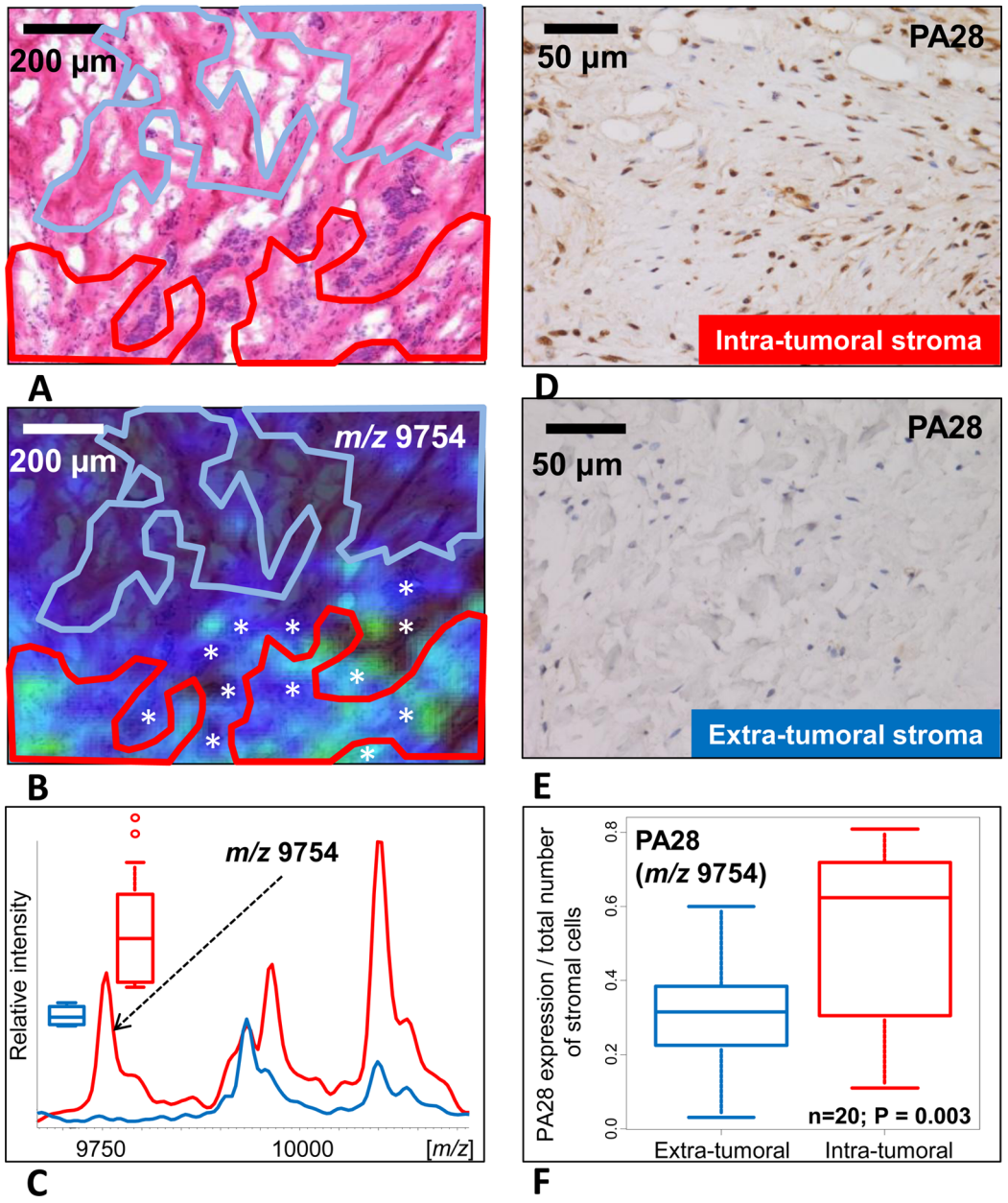

Figure 5. (A) H&E-stained image of a breast tumor that was analyzed via mass spectrometry imaging and the visualization of the *m*/*z* 9754 peak in the same area in panel B (the red and blue outlines show the intra- and extra-tumoral stroma, respectively; * signifies islands of tumor cells). (C) Boxplots of the overall difference of this peak. This finding was confirmed via immunohistochemistry, which confirmed that the staining for PA28 was increased in the intratumoral stroma (D) compared with the extratumoral stroma (E). (F) Boxplots for this difference.

al. cultured cancer-associated fibroblasts and normal stromal fibroblasts and identified 46 differentially expressed genes in the cancer-associated fibroblasts found in nonsmall cell lung cancer (NSCLC) compared with normal pulmonary fibroblasts.[18] This gene-signature was also of prognostic significance in independent NSCLC cohorts, further confirming the prognostic implications of stromal activation. These and similar experiments all examined differences at the mRNA level and only performed these analyses on stromal fibroblasts. Although fibroblasts are the predominant cell type within the tumor-associated stroma, these tissues also contain other cell types like pericytes, endothelium, inflammatory cells, and the structural proteins that form the extracellular matrix. Limiting the analysis to the cancer-associated fibroblasts might therefore leave several key properties of the tumor-associated stroma undetected.

MALDI MSI possesses unique characteristics for analyzing the molecular composition of cells within their natural environment. This nontargeted, label-free technique has established itself as a powerful method for the detection of biomolecular differences between and within tissues. To date, no MSI study has described differences in proteomic signatures between the tumor-associated stroma as a whole and normal physiologic stroma. In the current study, we have demonstrated that several differences in protein signatures exist between these two groups. Our analysis was based on the assumption that the proximity of the stromal tissues to the tumor cells is a major determinant of the activation of the tumor-associated stroma. Protein profiles were compared between stroma at a distance

dx.doi.org/10.1021/pr500253j | J. Proteome Res. 2014, 13, 4730−4738

from the tumor and the stroma that was directly adjacent to the tumor epithelium. It has been questioned whether such histologically normal extratumoral stromal tissues are in fact representative of normal stroma (i.e., that present in non-diseased breast tissues). Troester et al. have previously shown that stromal tissue at a distance from the tumor also display some degree of activation compared with reduction mammoplasty tissue,[19] despite the fact that the aspect of the stromal tissues distant from the tumor was histologically characterized as normal. Similar field effects have also been reported by MALDI MSI.[20,21] Even if the adjacent, histologically normal extratumoral stromal tissues used here as a control were subject to similar field effects, the protein biomarkers would still be indicative of the greater activation of the adjacent histologically activated tumor stroma and thus remain valid biomarkers for stromal activation.

Two of the three proteins that were detected and independently validated in our multicenter study, as being associated with activated stroma, have been previously identified.[12,13] The proteasome regulator PA28 (m/z_{Leiden} 9745 peak) has been shown to be increased in serous adenocarcinoma compared with normal ovarian tissue.[13] The detected ion is a fragment of the full-length 28 kDa protein PA28, which has been previously described to be a positive regulator of proteasome activity.[22] Inhibition of proteasome activity has been shown to lead to induction of apoptosis[23] and indicates that regulation of the proteasome is important in cancer tissues.

A cleaved version of thymosin β4 (m/z_{Leiden} 4570) was identified in our data sets to be specific to tumor-associated stroma (Figure 1B). The full-length thymosin β4 (m/z 4965) is a commonly detected protein in MALDI MSI experiments and was also detected here at much higher signal intensities than the cleaved form. Remarkably, there was no significant difference detected in the signal intensity of the full-length thymosin β4 in the intratumoral stroma compared with the extratumoral stroma for either the Munich or Leiden data sets. The full-length thymosin β4 protein has been reported to increase wound healing,[24] cellular proliferation, and angiogenesis[25] and is also known as an actin-sequestrating molecule. Similarly to PA28, no in vitro reports have described the functional consequences of this cleaved form of the molecule. Indeed one of the distinct advantages of intact protein MALDI MSI is its ability to uncover post-translational modifications in clinical tissues that would be missed using more established immunohistochemical assays or bottom-up proteomics approaches.

The protein signatures that we observed in this study were derived from two data sets that were independently recorded in two different centers and used two different tissue banks. To our knowledge, no studies have attempted to independently validate MSI results over multiple centers. Differences were observed in the spectra that were recorded in both centers, as would be expected considering the different sample preparation strategies employed.[10] Nevertheless, all protein ions that were found to be statistically significant in the Munich data set and that were also detected in the Leiden data set were also found to be statistically significant in the Leiden data set. Reassuringly, this also included proteins that were detected with lower signal intensities (cleaved form of thymosin β4).

The total-ion-count normalization used in this study can account for minor differences in MALDI MS performance due to inhomogeneous matrix coverage or laser intensity fluctuations[13] but cannot correct for the larger scale differences that may arise from differences in tissue processing and tissue preparation.[10] A reference tissue standard that matches the characteristics of the tissue (e.g., tissue from a xenograft mouse model of breast cancer) could be used as a quality control (QC) reference sample to ensure equivalent tissue preparation and mass spectrometry methods in the different centers. Explicit QC would enable rapid identification of unexpected sources of bias, as has been reported for MALDI based profiling of body fluids.[26] The increased scope for greater diversity in larger multicenter studies may make such QC essential for wider validation of MALDI MSI based assays.

Another important aspect concerns tissue selection because it is known that breast tumors are heterogeneous.[27] For both patient series (Munich and Leiden), diagnosis was first performed during routine pathological practice; teams of pathologists then selected and re-evaluated the tissues prior to their analysis to confirm diagnosis and subtype. Tissue selection and MALDI MSI data acquisition were performed entirely independently, and so the patient series were not matched for tumor subtype. All tissues were then carefully compared and examined to select tumor regions, activated stroma, and nonactivated stroma, which was overseen by trained pathologists from both locations (AW and VS). In this manner, the MALDI MSI data from histologically equivalent regions of tissue from independently selected and independently measured patient series could be compared. The independent validation of the stromal activation markers, in patients of different subtype, indicate that they may be generic markers of stromal activation. For more targeted clinical questions it will be important to first devise common patient selection criteria to ensure that identical subtypes are selected from all clinical centers.

5. CONCLUSIONS

In this study, MALDI MSI analysis performed over two centers identified robust proteomic signals associated with tumor-activated stromal tissues. Hierarchical clustering of proteomic profiles can distinguish the activated intratumoral stroma from the quiescent, extratumoral stroma. One of these markers (PA28) was also verified with IHC.

AUTHOR INFORMATION

Corresponding Author

*E-mail: L.A.Mcdonnell@lumc.nl. Phone: +31 71 526 8744. Fax: +31 71 526 6907.

Notes

The authors declare no competing financial interest.

ACKNOWLEDGMENTS

This work is financially supported by the Cyttron II project “Imaging Mass Spectrometry”, the COMMIT project e-biobanking, and the ZonMw Zenith project ‘Imaging Mass Spectrometry-Based Molecular Histology: Differentiation and Characterization of Clinically Challenging Soft Tissue Sarcomas.’ T.J.A.D. gratefully acknowledges the travel funding supplied by COST Action BM1104 for the Short Term Scientific Mission to the Helmholtz Zentrum München. B.D.B. is funded through Marie Curie Intra European Fellowship (No. 331866, SITH FP7-PEOPLE-2012-IEF). A.W. is supported by the Ministry of Education and Research of the Federal Republic of Germany (BMBF) (grant no. 0315505A, 01IB10004E) and

the Deutsche Forschungsgemeinschaft (SFB 824 TP Z02 and WA 1656/3-1).

■ ABBREVIATIONS

CAF, cancer-associated fibroblast; α-SMA, α-smooth muscle actin; MALDI-MSI, Matrix-assisted laser desorption/ionization mass spectrometry imaging; ToF, Time-of-flight; IHC, immunohistochemistry; TGF-β, transforming growth factor β; PDGF, platelet-derived growth factor; NSCLC, nonsmall cell lung cancer

■ REFERENCES

(1) Kalluri, R.; Zeisberg, M. Fibroblasts in cancer. *Nat. Rev. Cancer* **2006**, *6*, 392−401.
(2) Sugimoto, H.; Mundel, T. M.; Kieran, M. W. Raghu Kalluri Identification of fibroblast heterogeneity in the tumor microenvironment. *Cancer Biol. Ther.* **2006**, *5*, 1640−1646.
(3) Chaurand, P.; Sanders, M. E.; Jensen, R. A.; Caprioli, R. M. Proteomics in Diagnostic Pathology - Profiling and Imaging Proteins Directly in Tissue Sections. *Am. J. Pathol.* **2004**, *165*, 1057−1068.
(4) Cornett, D. S.; Reyzer, M. L.; Chaurand, P.; Caprioli, R. M. MALDI Imaging Mass Spectrometry: Molecular Snapshots of Biochemical Systems. *Nat. Methods* **2007**, *4*, 828−833.
(5) McDonnell, L. A.; Heeren, R. M. A. Imaging Mass Spectrometry. *Mass Spectrom. Rev.* **2007**, *26*, 606−643.
(6) Rauser, S.; Deininger, S.-O.; Suckau, D.; Höfler, H.; Walch, A. Approaching MALDI Molecular Imaging for Clinical Proteomic Research: Current State and Fields of Application. *Expert Rev. Proteomics* **2010**, *7*, 927−941.
(7) Reyzer, M. L.; Caldwell, R. L.; Dugger, T. C.; Forbes, J. T.; Ritter, C. A.; Guix, M.; Arteaga, C. L.; Caprioli, R. M. Early Changes in Protein Expression Detected by Mass Spectrometry Predict Tumor Response to Molecular Therapeutics. *Cancer Res.* **2004**, *64*, 9093−9100.
(8) Aichler, M.; Elsner, M.; Ludyga, N.; Feuchtinger, A.; Zangen, V.; Maier, S. K.; Balluff, B.; Schöne, C.; Hierber, L.; Braselmann, H.; Meding, S.; Rauser, S.; Zischka, H.; Aubele, M.; Schmitt, M.; Feith, M.; Hauck, S. M.; Ueffing, M.; Langer, R.; Kuester, B.; Zitzelsberger, H.; Höfler, H.; Walch, A. K. Clinical response to chemotherapy in oesophageal adenocarcinoma patients is linked to defects in mitochondria. *J. Pathol.* **2013**, *230*, 410−419.
(9) Seeley, E. H.; Lazova, R.; Sepehr, A.; Caprioli, R. M. In *Molecular Diagnosis of Atypical Spitzoid Neoplasms using Direct Tissue Profiling Mass Spectrometry*, 61st ASMS Conference on Mass Spectrometry and Allied Topics, Minneapolis, MN, USA, 2013.
(10) Goodwin, R. J. A. Sample preparation for mass spectrometry imaging: Small mistakes can lead to big consequences. *J. Proteomics* **2012**, *75*, 4893−4911.
(11) Cohen, S. L.; Chait, B. T. Influence of Matrix Solution Conditions on the MALDI-MS Analysis of Peptides and Proteins. *Anal. Chem.* **1996**, *68*, 31−37.
(12) Seeley, E. H.; Oppenheimer, S. R.; Mi, D.; Chaurand, P.; Caprioli, R. M. Enhancement of protein sensitivity for MALDI imaging mass spectrometry after chemical treatment of tissue sections. *J. Am. Soc. Mass Spectrom.* **2008**, *19*, 1069−77.
(13) Deininger, S. O.; Cornett, D. S.; Paape, R.; Becker, M.; Pineau, C.; Rauser, S.; Walch, A.; Wolski, E. Normalization in MALDI-TOF imaging datasets of proteins: practical considerations. *Anal. Bioanal. Chem.* **2011**, *401*, 167−181.
(14) Benjamini, Y.; Hochberg, Y. Controlling the false discovery rate: a practical and powerful approach to multiple testing. *J. R. Stat. Soc. B* **1995**, *57*, 289−300.
(15) Hardesty, W. M.; Kelley, M. C.; Mi, D.; Low, R. L.; Caprioli, R. M. Protein Signatures for Survival and Recurrence in Metastatic Melanoma. *J. Proteomics* **2011**, *74*, 1002−1014.
(16) McDonnell, L. A.; Walch, A.; Stoeckli, M.; Corthals, G. L. MSiMass List: A Public Database of Identifications for Protein MALDI MSI. *J. Proteome Res.* **2013**, *13*, 1138−1142.
(17) Longuespée, R.; Boyon, C.; Castellier, C.; Jacquet, A.; Desmons, A.; Kerdraon, O.; Vinatier, D.; Fournier, I.; Day, R.; Salzet, M. The C-terminal fragment of the immunoproteasome PA28S (Reg alpha) as an early diagnosis and tumor-relapse biomarker: evidence from mass spectrometry profiling. *Histochem. Cell Biol.* **2012**, *138*, 141−154.
(18) Navab, R.; Strumpf, D.; Bandarchi, B.; Zhu, C.-Q.; Pintilie, M.; Ramnarine, V. R.; Ibrahimov, E.; Radulovich, N.; Leung, L.; Barczyk, M.; Panchal, D.; To, C.; Yun, J. J.; Der, S.; Shepherd, F. A.; Jurisica, I.; Tsao, M.-S. Prognostic gene-expression signature of carcinoma-associated fibroblasts in non-small cell lung cancer. *Proc. Natl. Acad. Sci. U.S.A.* **2011**, *108*, 7160−7165.
(19) Troester, M. A.; Lee, M. H.; Carter, M.; Fan, C.; Cowan, D. W.; Perez, E. R.; Pirone, J. R.; Perou, C. M.; Jerry, D. J.; Schneider, S. S. Activation of Host Wound Responses in Breast Cancer Microenvironment. *Clin. Cancer Res.* **2009**, *15*, 7020−7028.
(20) Caldwell, R. L.; Gonzalez, A.; Oppenheimer, S. R.; Schwartz, H. S.; Caprioli, R. M. Assessment of the Tumor Protein Microenvironment Using Imaging Mass Spectrometry. *Cancer Genomics Proteomics* **2006**, *3*, 279−288.
(21) Oppenheimer, S. R.; Mi, D.; Sanders, M. E.; Caprioli, R. M. Molecular Analysis of Tumor Margins by MALDI Mass Spectrometry in Renal Carcinoma. *J. Proteome Res.* **2010**, *9*, 2182−2190.
(22) Ahn, K.; Erlander, M.; Leturcq, D.; Peterson, P. A.; Früh, K.; Yang, Y. In vivo characterization of the proteasome regulator PA28. *J. Biol. Chem.* **1996**, *271*, 18237−18242.
(23) Chen, D.; Landis-Piwowar, K. R.; Chen, M. S.; Dou, Q. P. Inhibition of proteasome activity by the dietary flavonoid apigenin is associated with growth inhibition in cultured breast cancer cells and xenografts. *Breast Cancer Res.* **2007**, *9*, R80.
(24) Malinda, K.; Sidhu, G.; al, M. H. e. Thymosin beta4 accelerates wound healing. *J. Invest Dermatol.* **1999**, *113*, 364−368.
(25) Cha, H.-J.; Jeong, M.-J.; Kleinman, H. K. Role of Thymosin β4 in Tumor Metastasis and Angiogenesis. *J. Natl. Cancer Inst* **2003**, *95*, 1674−1680.
(26) Villanueva, J.; Philip, J.; Chaparro, C. A.; Li, Y.; Toledo-Crow, R.; DeNoyer, L.; Fleisher, M.; Robbins, R. J.; Tempst, P. Correcting Common Errors in Identifying Cancer-Specific Serum Peptide Signatures. *J. Proteome Res.* **2005**, *4*, 1060−1072.
(27) Stephens, P. J.; Tarpey, P. S.; Davies, H.; Loo, P. V.; Greenman, C.; Wedge, D. C.; Nik-Zainal, S.; Martin, S.; Varela, I.; Bignell, G. R.; Yates, L. R.; Papaemmanuil, E.; Beare, D.; Butler, A.; Cheverton, A.; Gamble, J.; Hinton, J.; Jia, M.; Jayakumar, A.; Jones, D.; Latimer, C.; Lau, K. W.; McLaren, S.; McBride, D. J.; Menzies, A.; Mudie, L.; Raine, K.; Rad, R.; Chapman, M. S.; Teague, J.; Easton, D.; Langerød, A.; The Oslo Breast Cancer Consortium (OSBREAC); Lee, M. T. M.; Shen, C.-Y.; Tee, B. T. K.; Huimin, B. W.; Broeks, A.; Vargas, A. C.; Turashvili, G.; Martens, J.; Fatima, A.; Miron, P.; Chin, S.-F.; Thomas, G.; Boyault, S.; Mariani, O.; Lakhani, S. R.; Vijver, M. v. d.; AVeer, L. v. t.; Foekens, J.; Desmedt, C.; Sotiriou, C.; Tutt, A.; Caldas, C.; Reis-Filho, J. S.; Aparicio, S. A. J. R.; Salomon, A. V.; Børresen-Dale, A.-L.; Richardson, A. L.; Campbell, P. J.; Futreal, P. A.; Stratton, M. R. The landscape of cancer genes and mutational processes in breast cancer. *Nature 486*, 400−404.